Damage Accumulation in Mild Steel Specimens under Mode I, Mode II and Mixed Mode I-II Loading Conditions

Botvina L. [a], Soldatenkov A. [b] and Tyutin M. [c]

Baikov Institute of Metallurgy and Material Sciences, Russian Academy of Sciences, Leninsky Avenue, 49, Moscow 119991, Russia

[a] botvina@imet.ac.ru, [b] alexxx.soldatenkov@yandex.ru, [c] tyutin@imet.ac.ru

Keywords: mixed-mode loading, plastic zones, acoustic emission, shear lips.

Abstract. The influence of the shear load component on the evolution of plastic zones, mechanical and acoustic properties of mild steel specimens is studied. It was found that an increase in the contribution of the shear component of loading leads to following changes: a decrease in the area of plastic zone and the shear lip size; the appearance of an additional system of microcracks, which results in an increase in the number of both microcracks and acoustic emission signals; an increase of the total fracture energy and the *J*-integral; a reduction in the slopes of the cumulative number distributions of both acoustic signal amplitudes and microcrack lengths, which characterize the fracture probability and used for its prediction.

Introduction

Service life prediction of structures and their elements is the main problem of fracture mechanics. To solve this problem, it is necessary to know the laws of damage localization and its development under different loading conditions and on different stages. Although these issues are paid a sufficient attention, most studies have focused on either modeling damage accumulation process or the theoretical solution of specific applications. The conceptions of the damage localization and the formation of plastic zones developed nearly half a century ago [1, 2] and also early experimental studies of plastic zones [3–5] are used in these investigations. At the same time there are very little works devoted to quantitative assessments of material damage in the plastic zone at mixed modes of loading, i.e. under conditions of tensile and shear component combination. However, the need of such an assessment for the development of methods of nondestructive testing and optimizing the structure of the material is obvious. This work was performed in order to fill this gap. The mechanical and physical behavior of mild structural steel under tension (mode I), in-plane shear (mode II) and mixed mode I-II loading conditions with the registration of acoustic emission (AE) was investigated. The size of plastic zones and the value of *J*–integral were estimated and the multiple fracture patterns in the plastic zones were studied.

Material and methods

Single edge notch specimens ($140 \times 80 \times 4$ mm) from mild steel with the ferritic–pearlitic structure were used (Fig. 1a). The average grain size is 30 μm. Standard mechanical properties of material under investigation are as follows: yield strength $\sigma_{0,2} = 282$ MPa; ultimate tensile strength $\sigma_{ult} = 434$ MPa and elongation at failure $\delta = 40$ %. Mixed mode I-II loading was created using special loading devices proposed in [6]. These loading devices allow to get mode I, mode II and mixed mode I-II loading in a conventional uniaxial testing machine applying tensile force through different holes (Fig. 1b), i.e. varying angle β between line of the notch and loading direction. All the fracture tests were carried out at room temperature using Instron 3382 testing machine at a constant displacement rate of 0.5 mm/min.
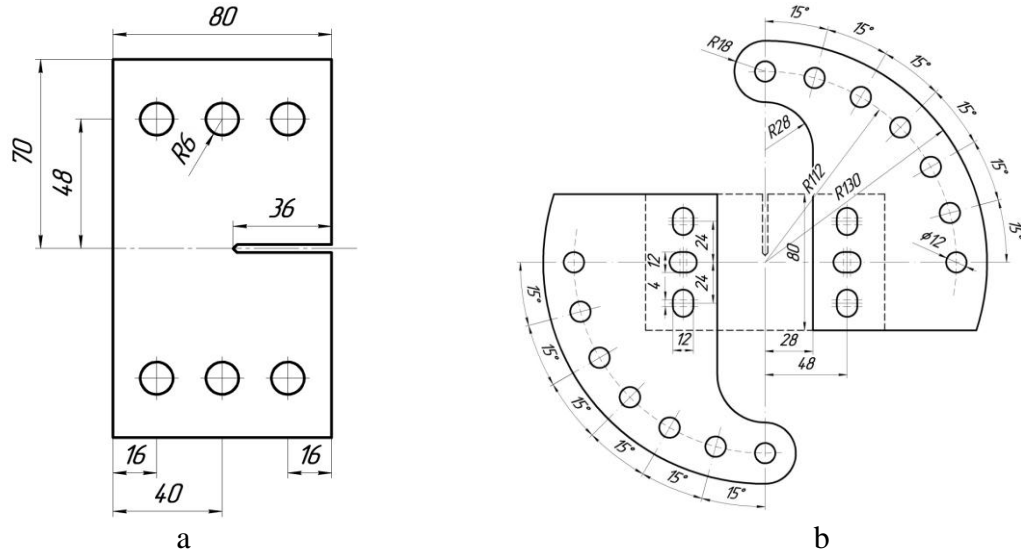
Fig. 1. (a) The geometry of the specimen for static tests under mode I, mode II and mixed mode I-II loading conditions; (b) the specimen in loading devices suggested by Richard [6]

The following parameters were evaluated from graphs of load versus displacement: the maximum load ($P_{\max}$); the maximum stress in cross-section of specimen ($\sigma_{\max}^n$); the area under load–displacement curve that corresponds to the total fracture energy (S_{Σ}); the areas under the curve before (S_1) and after (S_2) achievement of $P_{\max}$ that were assumed to be the crack initiation and propagation energies, respectively; and the relative difference of these energies, $(S_2 - S_1)/S_{\Sigma}$.

The stress intensity factors (SIFs) for mode I (K_I), mode II (K_{II}) and the effective SIF (K_{eff}) were calculated according to the following equations [7]:

$$K_I = Y_I \cdot P\sqrt{\pi l} , \tag{1}$$

$$K_{II} = Y_{II} \cdot P\sqrt{\pi l} , \tag{2}$$

$$K_{eff} = \sqrt{K_I^2 + K_{II}^2} , \tag{3}$$

where Y_I, Y_{II} – the correction factors, P – the load, l – the crack length.
In addition, the values of J–integral at different stages of loading were estimated on the work of plastic deformation. The dependencies of this parameter on the relative load were plotted.

$$J = \frac{A_p}{(W - l)t} , \tag{4}$$

where A_p – the work of plastic deformation estimated as area under the load–displacement curve at different stages before achievement of $P_{\max}$, W, t – the specimen width and thickness, respectively.
During loading the acoustic emission (AE) signals were recorded by means of four-channel system InterUnis A-Line 32D in the frequency range of 50-500 kHz using piezoelectric detectors that have resonance at frequency of 150 kHz. The amplitude threshold was set equal to 32 dB. The number of AE signals (N_{AE}) and acoustic activity ($dN_{AE}/d\tau$) were estimated. In addition, the b_{AE}–values were

assessed [8], i.e. the slope in the relation between the total number and amplitude of AE signals. For this purpose the graphs of the cumulative number distribution of AE amplitudes were plotted in the coordinate axes $\Sigma N_{AE} - A$, where ΣN_{AE} – the cumulative number of AE signals with amplitude not less than given one, A – the signal amplitude in dB.

The b_{AE}–values were determined from the following relation

$$20 \cdot \lg \Sigma N_{AE} = C - b_{AE} \cdot A. \tag{5}$$

The number of events for the determination of the b_{AE}–value was not less than 200.

In order to study plastic zones, the silicon replicas were removed from the polished lateral surface of a specimen on different stages of loading. The replicas were analyzed with an optical microscope Olympus GX 51 equipped with a video camera. The multiple fracture patterns were investigated on the lateral surfaces of broken specimens at different distances from the fracture surface. Microcrack distributions and sizes of plastic zones were assessed using digital image postprocessing program Atlas Tescan. The width, length and area of plastic zones, the b_C–parameter of microcrack distributions [9] and the k–parameter (concentration criterion) [10] were estimated.

Exponential and power relations were used for calculation of the b_C–parameter:

$$\Sigma N_C = Const \cdot \exp\left(-b_C \cdot l\right) \tag{6}$$

and

$$\Sigma N_C = Const \cdot l^{-b_C}, \tag{7}$$

where ΣN_C is the cumulative number of microcracks with length not less than given one. Parameter k was determined from the following equation:

$$k = \frac{1}{l_{av}\sqrt{\rho_C}}, \tag{8}$$

where l_{av} and ρ_C – the average length and density of microcracks, respectively.

Results

Typical load versus time curves obtained under tensile ($\beta = 90\,°$) and shear ($\beta = 0\,°$) loading conditions are shown in Fig. 2. In addition, the dependence of AE activity on time is present in Fig. 2. According to these data, the maximum load and the area under load-displacement curve (i.e. the total fracture energy) obtained under mode II loading conditions are higher than values of these characteristics assessed in tension. The increase in plasticity of the material under shear conditions may be the possible reason of such trend. It is confirmed by a J-integral assessment at the different loading stages. Indeed, the value of this parameter is significantly higher for mode II and mixed mode I-II loading than for pure mode I (Fig. 3a).
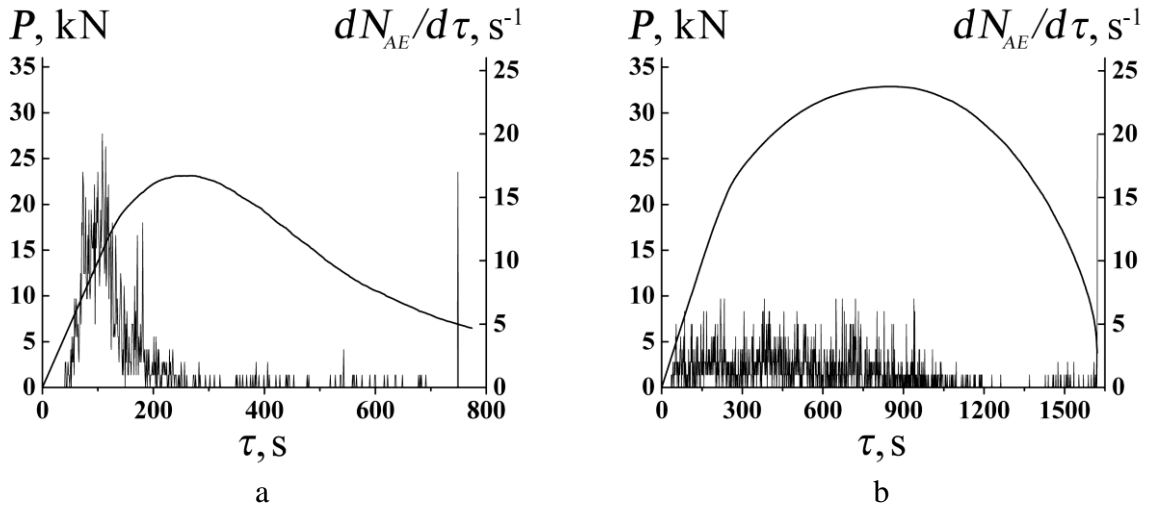
Fig. 2. The load versus time curves with superimposed AE activity data for mode I (a) and mode II (b) loading

At the same time the increase in part of shear stress component (i.e. reduction of the angle β) results in decrease in effective stress intensity factor K_{eff} (Fig. 3b). It may be connected to a lower crack growth resistance under shear loading conditions.
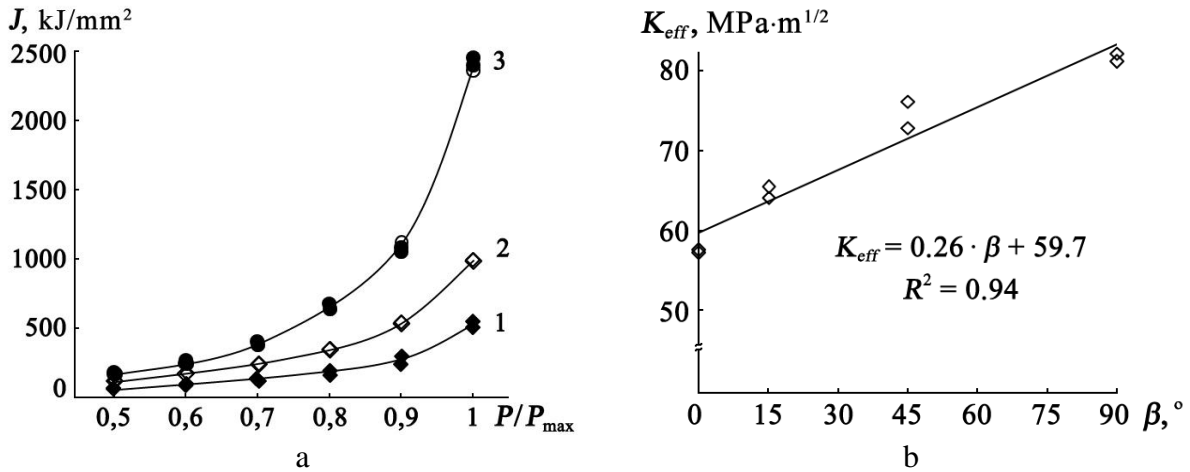
Fig. 3. (a) The values of J-integral characterizing fracture energy at different loading stages under mode I (1), mixed mode, $\beta = 45$ °, (2) and mode II loading conditions. (b) The dependence of K_{eff} on the angle β between line of the notch and loading direction.

Analysis of the fracture surfaces revealed that less ductility was observed for specimens tested under conditions of shear compared with those of tension. The reason of such contradiction became clear after comparison of the macrocrack initiation and propagation energies (S_1 and S_2, respectively). It appeared from this that S_2 is larger than S_1 for mode II as compared with mode I loading. However, the relative difference value of these energies, $(S_2 - S_1)/S_\Sigma$, is less for shear loading conditions (Table 1 and Fig. 4a). In addition, macrorelief of fracture surfaces of specimens tested in shear was more brittle in comparison with that of tensile specimens, since the size of shear lips, λ, and their relative values, λ/t, are lower (Fig. 4b).
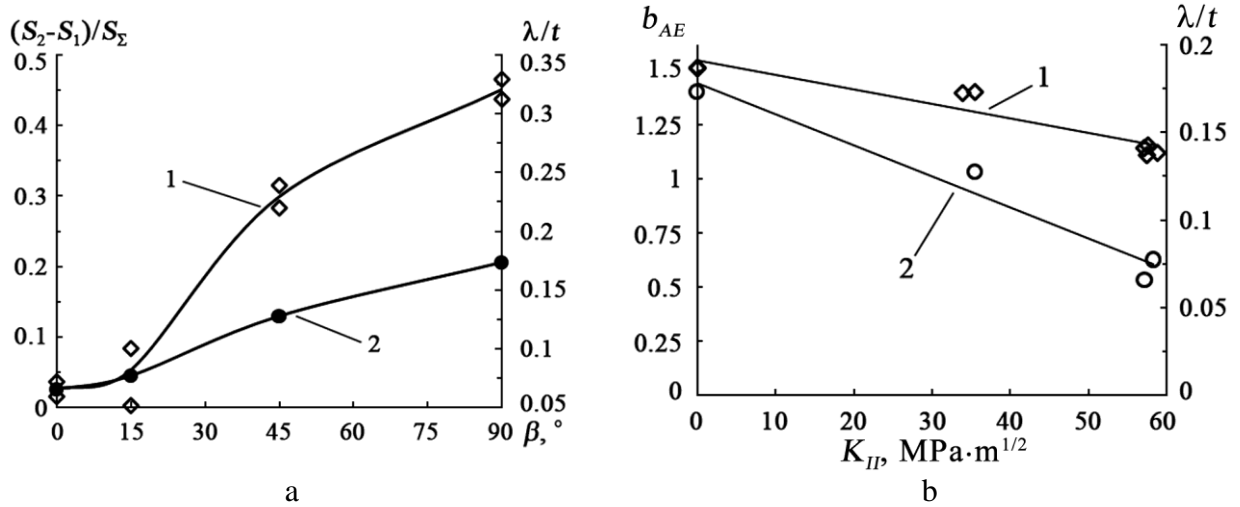
Fig. 4. (a) Dependencies of $\left(S_2 - S_1\right)/S_\Sigma$ (1) and λ/t (2) on angle β between line of the notch and loading direction. (b) Dependencies of the b_{AE}–value (1) and λ/t (2) on mode II stress intensity factor K_{II}.

Table 1. Mechanical and acoustic properties of tested specimens

β, °	b_{AE}	ΣN_{AE}	P_{max} [kN]	σ_{max}^n [MPa]	S_1 [J]	S_2 [J]	$\left(S_2 - S_1\right)/S_\Sigma$	K_I [MPa·m$^{1/2}$]	K_{II} [MPa·m$^{1/2}$]	K_{eff} [MPa·m$^{1/2}$]
90	1.51	548	23.4	167.4	37.7	96.4	0.44	81.10	0	81.1
90	1.52	1276	23.1	169.2	34.7	95.1	0.46	82.1	0	82.1
45	1.40	915	27.9	202.0	68.8	123.2	0.28	67.3	35.5	76.1
45	1.40	622	26.3	193.3	67.1	128.8	0.31	64.3	33.9	72.7
15	1.12	969	25.8	197.7	154.1	155.0	0.003	27.9	57.6	65.4
15	1.16	3330	32.1	243.0	177.9	210.5	0.08	28.5	58.9	64.0
0	1.11	1627	32.9	233.1	173.3	161.0	0.04	0	57.5	57.5
0	1.14	1523	29.4	230.4	152.9	157.8	0.02	0	57.1	57.1

The mode II fracture of specimens is accompanied by an increase in the total number of AE signals (see Table. 1 and Fig. 2). Evaluation of b_{AE}–parameter according to Eq. 1 that characterizes the total acoustic activity showed that for shear loading this parameter decreases (see Table 1), i.e. the number of signals with higher amplitude increases. Taking into account the presented data, this means that the b_{AE}–parameter decreases with increase in both maximum stress, σ_{max}^n, in the net section of a specimen and mode II stress intensity factor, K_{II}. In the last case the scatter of experimental data becomes less (Fig. 4b). The dependence of relative values of shear lip size, λ/t, observed on fracture surfaces on the mode SIF, K_{II}, has the same trend.

The increase in shear stress component leads to changes of both the plastic zone shape in the specimen notch tip at the identical values of P/P_{max} (Fig. 5) and multiple fracture patterns in the zones (Fig. 6). The area and width of plastic zones decrease but their length increases under shear conditions. It results from a greater localization of plastic deformation under shear conditions that

causes decrease in effective stress intensity factor for mode II loading and crack growth without sufficient plastic deformation.
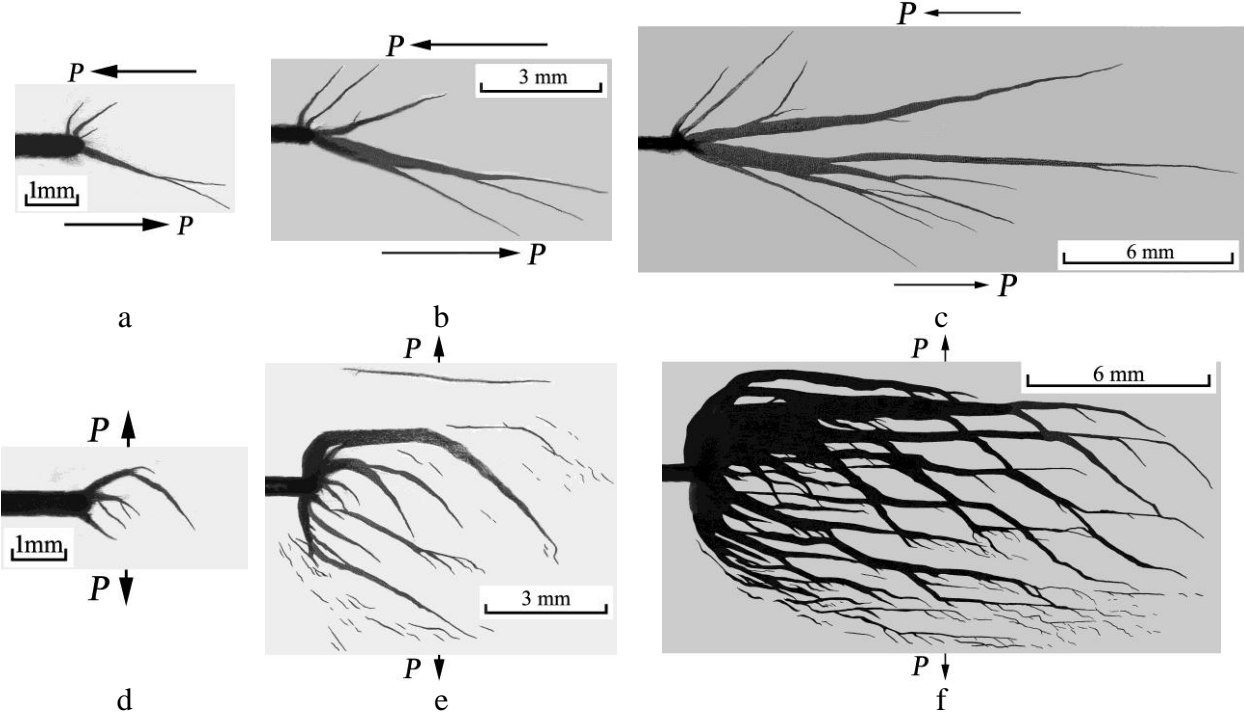
Fig. 5. The plastic zones at the notch tips of specimens from mild steel under in-plane shear (a–c) and tension (d–f) on the different stages at relative loads, P/P_{max} , equal to 0.2 (a, d), 0.4 (b, e) and 0.6 (c, f). The arrows indicate the direction of load application.
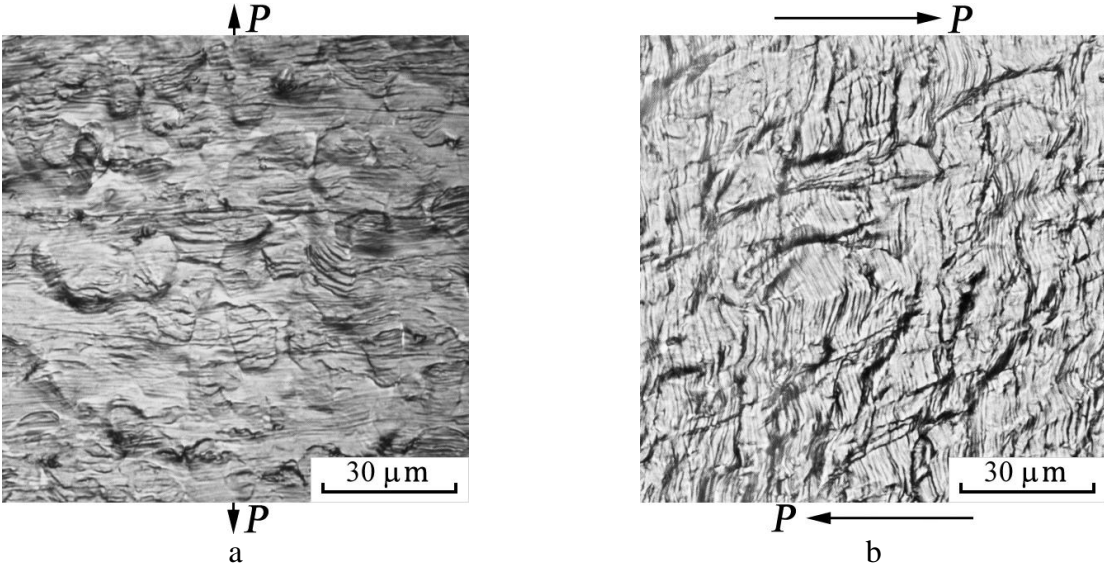
Fig. 6. The multiple fracture patterns in the plastic zones under tension (a) and shear (b). The arrows indicate the direction of load application.

It is worth noting one more fracture feature of specimens tested under shear. An additional microcrack system appears that has orientation at some angle to loading direction and causes increase in the total number of microcracks (Fig. 6 and Table 2). At the same time the average length and density of microcracks grow. These changes indicate a greater damage of material within plastic zone at shear and affect the cumulative number distributions of microcrack lengths resulting in decrease in the b_C– and k–parameters. This decrease is consistent with reduction of the b_{AE}–value under shear loading.

Table 2. Characteristics of multiple fracture patterns within plastic zones under tensile and shear loading conditions

	L_{av} [μm]	ΣN_C	ρ_C [μm^{-2}]	k	b_C
Mode I (Fig. 6a)	4,1	312	0,025	1,55	0,33
Mode II (Fig. 6b)	6,1	641	0,05	0,72	0,1

Discussion
Our results demonstrate that the damage accumulation under mode II loading is larger than that under mode I loading. This have an effect on the damage parameters estimated.
The data of the present work are confirmed by the studies [11, 12]. Indeed, the authors of [11] investigated the damage zones in the notched specimens from the rubber-modified epoxy resin tested under mode I and mixed-mode I-II loading conditions and found the plastic zone restriction on the specimen surface with increase in shear stress component. It is consistent with the changes in the plastic zone shape and size observed in the present study.
The decrease in the b_{AE}–value at shear loading was observed in [12] where the seismic activity in five different regions was analyzed.
The revealed changes in the acoustic emission parameters may be used when developing the nondestructive methods of fracture analysis.
Thus, our results demonstrate that the decrease in estimated damage parameters may be due to not only the damage coalescence and the formation of larger cracks, but also a change in the loading mode, i.e., transition from mode I to mode II conditions.

Conclusions
An increase in shear stress component leads to the following changes in the mechanical and physical behavior of mild steel:
  – the shape of plastic zone at the notch tip;
  – an appearance of additional microcrack system;
  – the increase in the total fracture energy and J–integral, but decrease in the relative difference between the crack initiation and propagation energies;
  – the reduction in the relative values of shear lip sizes on the fracture surfaces of specimens;
  – the decrease in damage parameters (b_{AE}, b_C, and k);
  – the reduction in the b_{AE}–value with increase in mode II stress intensity factor.

References

[1]   D.S. Dugdale. *Yielding of Steel Sheets Containing Slits.* J. Mech. Phys. Solids, 1960, Vol. 8, No. 2, pp. 100–104.

[2]   G.R. Irwin. *Plastic Zone near a Crack and Fracture Toughness.* Proc. 7th Sagamore Ordinance Mater. Res. Conf. NY: Syracuse University Press. Vol. 4, pp. 63–77.

[3]   G.T. Hahn, A.R. Rosenfield. *Local yielding and extension of a crack under plane stress.* Acta Metallurgica, 1965, Vol. 13, No. 3, pp. 293–306.

[4]   G.T. Hahn, R.G. Hoagland, A.R. Rosenfield. *Local yielding attending fatigue crack growth.* Metall. Mater. Transact., 1972, Vol. B3, No. 5, pp. 1189–1202.

[5]   T. Yokobori, K. Sato, H. Yaguchi. *Observations of Microscopic Plastic Zones and Slip Band Zone at the Tip of a Fatigue Crack.* Reports of the Research Institute for Strength and Fracture of Materials (Tohoku University, Sendai, Japan), 1973, Vol. 9, No. 1, pp. 1–10.

[6]   H.A. Richard, K. Benitz. *A loading device for the creation of mixed mode in fracture mechanics.* Int. J. Fract., 1983, Vol. 22, No. 2, pp. R55–R58.

[7]   D. Broek. *Elementary engineering fracture mechanics.* Leyden, 1974.

[8]   L.R. Botvina, T.B. Petersen, M.R. Tyutin. *Estimation and Analysis of b-Value of Acoustic Emission.* Zavod. Lab., Diagn. Mater., 2011, No. 3.

[9]   L.R. Botvina, N.A. Zharkova, M.R. Tyutin, T.B. Petersen, V.G. Budueva. *Kinetics of Damage Accumulation in Low-Carbon Steel under Tension.* Deformatsiya i Razrushenie Materialov, 2005, No. 3, pp. 2–8.

[10] S.N. Zhurkov, V.S. Kuksenko, A.I. Slutsker. *Formation of Submicroscopic Fractures in Polymers under Loading.* Fizika Tv. Tela, 1969, Vol. 11, No. 1, pp. 296–302.

[11] D.B. Lee, T. Ikeda, N. Miyazaki, N.S. Choi. *Damage zone around crack tip and fracture toughness of rubber-modified epoxy resin under mixed-mode conditions.* Eng. Fract. Mech., 2002, Vol. 69, No. 12, pp. 1363–1375.

[12] D. Schorlemmer, S. Wiemer, M. Wyss. *Variations in earthquake-size distribution across different stress regimes.* Nature, 2005, Vol. 437, N. 7058, pp. 539–542.